ELSEVIER

Polymer 41 (2000) 4709–4717

polymer

Synthesis and rheological investigation on phase behaviors of semiflexible type amorphous liquid crystalline poly(ester-imide)s

S.O. Kim, T.K. Kim, I.J. Chung*

Department of Chemical Engineering, Korea Advanced Institute of Science and Technology, 373-1 Kusong, Yusong, Taejon 305-701, South Korea

Received 19 July 1999; received in revised form 10 September 1999; accepted 15 September 1999

Abstract

Main chain type thermotropic poly(ester-imide)s composed of *N*-(ω-carboxyalkylene) trimellitic imides and methylhydroquinone diacetate or hydroquinone diacetate were prepared by melt transesterification condensation. DSC and polarized light microscopy observation revealed that polymers made from hydroquinone diacetate showed both crystal melting and mesophase to isotropic phase transition but those from methylhydroquinone diacetate showed only mesophase to isotropic phase transition. The amorphous type liquid crystalline polymers showed extremely slow crystallization velocities. The mesophase of all polymers was verified as a nematic one from the drops of moduli and viscosities at the isotropic to mesophase transition during cooling. For an amorphous liquid crystalline polymer the changes of dynamic rheological properties were checked around the mesophase to isotropic phase transition. Both isotropic and nematic phases succeeded in time–temperature superposition but biphase failed.

Keywords: Thermotropic; Poly(ester-imide); Phase transition

1. Introduction

The main chain type thermotropic polymers have been extensively studied. In the early days studies on thermotropic polymers were motivated to develop the materials with high mechanical properties. Such industrial interests were mainly focused on rigid rod-type copolymers and their blends with conventional polymers. On the other hand much academic research has also been performed to understand the characters of the thermotropic polymers. Most of them paid attention to semiflexible polymers, in which the hard mesogenic groups are connected by flexible spacer groups. Until now, enormous semiflexible type thermotropic polymers have been synthesized. The typical examples are polyesters [1–5], poly(ester-amide)s [6], polyethers [7,8], etc. Recently, various thermotropic poly(ester-imide)s have been synthesized by Kricheldorf et al. (Ref. [9] and references therein). The poly(ester-imide)s having the regular sequence of flexible spacer and aromatic group showed smectic mesophases because of the great difference in polarity between the aliphatic spacer and aromatic imide.

In a previous publication, we prepared poly(ester-imide)s and copoly(ester-imide)s from *N*-(ω-carboxyalkylene) trimellitic imides and 2,6-diacetoxynaphthalene [10]. All polymers showed nematic mesophase due to the asymmetry of imide containing monomer units. In addition, the copoly(ester-imide)s showed extremely slow crystallization behaviors. Nematic glassy phase could be obtained under the usual cooling conditions. Such amorphous thermotropic polymers are useful materials to study the physical properties, especially rheological properties, of liquid crystalline phase of polymers, because they show wide mesophase temperature range in the experimental time [10–18]. In this present article we prepared poly(ester-imide)s from same imide containing monomer with hydroquinone diacetate or methylhydroquinone diacetate. The phase behaviors of polymers are characterized and discussed from the viewpoint of molecular structures. The effects of the phase status on the rheological properties are tested by dynamic rheological measurements. It has to be noted that poly(ester-imide)s made from *N*-(ω-carboxyalkylene) trimellitic imides with hydroquinone diacetate were synthesized by Kricheldorf et al. before [19]. But their characteristics were not reported precisely. We checked their phase behavior to compare with those of the polymers made from methylhydroquinone.

2. Experimental

2.1. Materials

Trimellitic anhydride, 5-aminovaleric acid, 2-azacyclooctanone, hydroquinone and methylhydroquinone were

* Corresponding author. Tel.: +82-42-869-3916; fax: +82-42-869-3910.
E-mail address: chung@cais.kaist.ac.kr (I.J. Chung).

0032-3861/00/$ - see front matter
PII: S0032-3861(99)00666-7

purchased from Aldrich Chemical Co. Hydroquinone and methyl hydroquinone were acetylated by means of acetic anhydride in boiling toluene with the catalytic amount of pyridine. *N*-(4-carboxybutyl) trimellitic imide was synthesized from 5-aminovaleric acid and trimellitic anhydride by chemical imidization reaction in DMF with toluene. *N*-(6-carboxyhexyl) trimellitic imide was synthesized from 2-azacyclooctanone and trimellitic anhydride by high temperature condensation reaction without solvents.

2.2. Polymerization

Poly(ester-imide)s were polymerized by melt transesterification reaction with MgO catalyst. Reaction condition is similar to that of Kricheldorf et al. [19]. The reactants were heated to 220°C, where the condensation started, under nitrogen atmosphere. The temperature was raised to 270°C in step wise manner and at last stage they were condensed at 270°C for 1 h under vacuum to eliminate acetic acid and low molecular weight condensates. For the case of methyl hydroquinone diacetate 10% excess amount was added because of sublimation.

2.3. Measurements

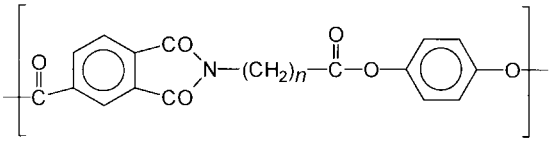

4H (n=4) and 6H (n=6)

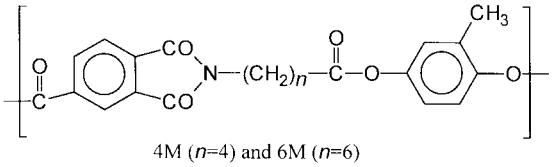

4M (n=4) and 6M (n=6)

The solution of 60 mg poly(ester-imide)s in 600 μl deuterated trifluoroacetic acid was used for the measurement of ^{13}C NMR (Bruker, AMX FT 500 MHz) spectra of poly (ester-imide)s. Inherent viscosity was measured in *m*-cresol and NMP at the concentration of 0.5 g/dl. A polarized light microscope (PLM, A Leitz, Model Laborlux 12 Pols) coupled with a Mettler FP-2 hot stage was used to observe the mesophase textures of all poly(ester-imide)s. Thermal transition studies were carried out with Perkin–Elmer DSC 2 and du Pont 2010 Thermal Analyzer under nitrogen atmosphere. Wide angle X-ray diffractograms (WAXD) were obtained using Rigaku X-ray generator (CuKα_1 radiation with $\lambda = 0.15406$ nm). Film type samples were rotated to exclude the effect of local orientation. Scan speed was 2°/min. Temperature sweep measurements of viscoelastic properties were conducted with PHYSICA RheoLab MC 120 dynamic rheometer. 50 mm parallel plate geometry was used for disk shape molded samples. Strain was 0.1 for the temperature sweep measurements. Dynamic frequency sweep measurements were performed on ARES rheometer with 25 mm parallel plate geometry. All measurements were done in the linear viscoelasticity.

3. Results and discussion

3.1. Synthesis

The chemical structures of all synthesized polymers are verified with ^{13}C NMR measurements. 125 MHz ^{13}C NMR spectrum and the assignment results of 4M are shown in Fig. 1. Because *N*-(ω-carboxyalkylene) trimellitic imides and methylhydroquinone diacetates have asymmetrical chemical structures, the synthesized polymers have copolymeric character. The peaks of ester carbonyl carbons split into a doublet owing to the asymmetrical chemical structures of methylhydroquinone diacetate. When the symmetric naphthalene or hydroquinone units were used, the carbonyl carbon peaks appeared as a singlet [10]. The split two peaks showed almost the same intensity, which means that the reactivity of acid groups with acetates of methylhydroquinone diacetates is almost equal. From the results of ^{13}C NMR measurements and features of transesterification polycondensation process, the synthesized polymers can be regarded as random copolymers.

Table 1 presents the inherent viscosities of all prepared polymers measured in the solutions of *m*-cresol and NMP. *m*-cresol dissolves all polymers but NMP dissolves only polymers made from methylhydroquinone diacetate. We can find that the inherent viscosities of the polymers containing hexamethylene units are higher than those containing four methylene units. Similar results were reported by Kricheldorf et al. [19]. But they used a different synthetic scheme for the synthesis of 6H.

3.2. Thermal transition behaviors

Fig. 2 shows the DSC traces of 4H and 6H. For an as polymerized sample, first heating, cooling and second heating were conducted. All scanning rates were 10°C/min. One can find a glass transition at 83°C and two endothermic transitions at 221 and 268°C in the second heating trace of 4H. Because the polymer degraded rapidly after the second endothermic transition, the cooling run was started from the temperature between the two endothermic transitions. An exothermic transition is seen at 167°C during cooling and the heat of fusion (0.69 kcal/mru) of the exotherm matches very well with that of the low temperature endotherm on the second heating. Large supercooling behavior of the transition means that the endotherm of heating process is crystal melting and the exotherm of cooling is the corresponding crystallization.

For 6H, the temperature ranges of all endotherms are far below the degradation temperature. The cooling and second

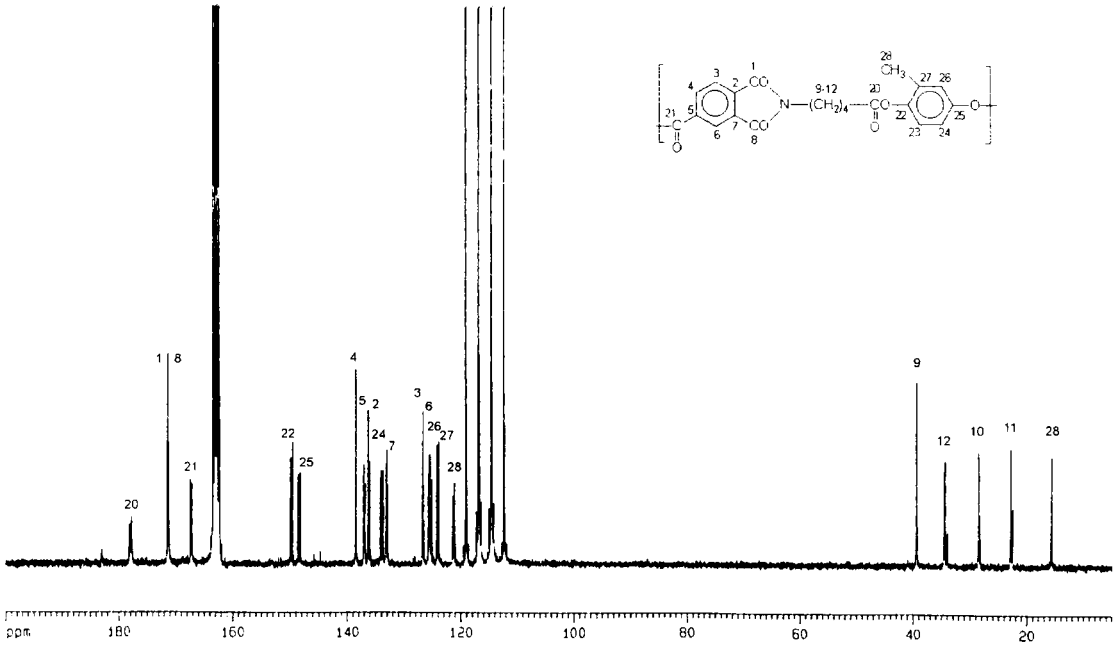

Fig. 1. 125 MHz ^{13}C NMR spectrum of 4M.

heating scans are shown. One can find a glass transition at 73°C and two major endothermic transitions at 221 and 255°C on heating scan and two exothermic transitions at 245 and 192°C in the subsequent cooling scan. The peak temperature of higher temperature exotherm is very close to that of the corresponding endotherm of heating scan. But the lower temperature exotherm locates 20°C below the lowest (minor) endotherm on heating. The little supercooling behavior of higher temperature endotherm is a feature of low ordered mesophase transition [20].

4M and 6M revealed very different results from 4H or 6H on DSC scans at similar scan rates (Fig. 3). For 4M, glass transition at 76°C and only one endotherm at 230°C are observed during heating scan. Cooling scan reveals a corresponding exotherm at 222°C. The results of 6M are similar to those of 4M. A glass transition at 61°C and an endotherm at 186°C are observed on heating and an exotherm at 175°C is observed on cooling. The endothermic processes of both polymers show little supercooling behaviors during cooling.

To check the mesophase formation, all polymers were observed on polarized light microscopy. Upon heating, 4H shows mobile mesophase texture above the crystal melting temperature on DSC. The morphology became isotropic crossing the temperature of the higher temperature endotherm, which means the mesophase to isotropic phase transition. In the following cooling process, the mesophase texture showed little changes during cooling but did not flow when externally sheared below the crystallization temperature. The textural change of 6H with temperature is similar with that of 4H. But biphasic texture rather than

Table 1
Inherent viscosities of all prepared poly(ester-imide)s

Polymer	η_{inh} (dl/g)[a]	η_{inh} (dl/g)[b]
4H	0.249	Insoluble
6H	0.607	Insoluble
4M	0.583	0.25
6M	0.762	0.33

[a] Measured in *m*-cresol with $c = 0.5$ g/dl at 20°C.
[b] Measured in NMP with $c = 0.5$ g/dl at 20°C.

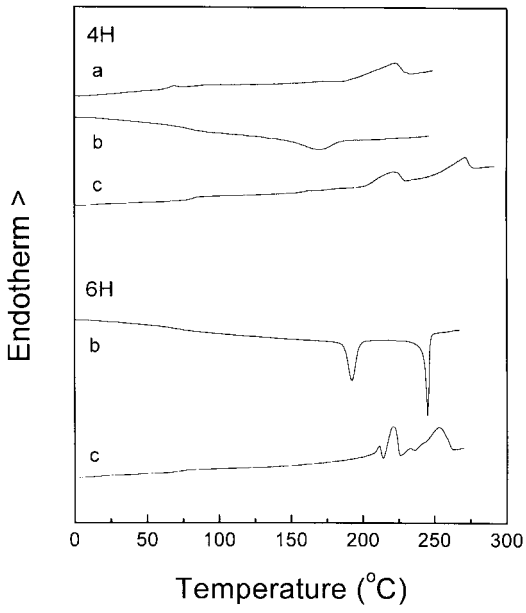

Fig. 2. DSC thermograms of 4H and 6H at scan rates of 10°C/min: (a) first heating of as polymerized sample; (b) cooling; and (c) second heating.

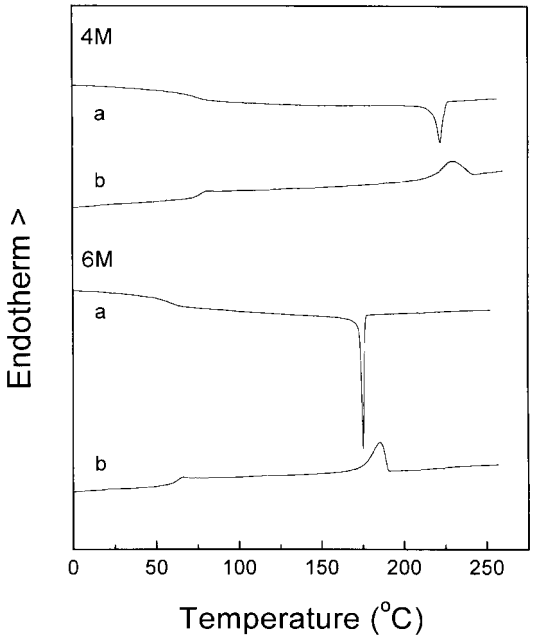

Fig. 3. DSC thermograms of 4M and 6M at scan rates of 10°C/min: (a) cooling; and (b) second heating.

fully developed mesophase was observed after crystal melting. Mesophase textures are also observed for 4M and 6M. The DSC endothermic transitions of both polymers are verified as mesophase to isotropic phase transitions on polarized light microscopy. Polarized light micrographs of mesophase and biphasic textures of 4M are shown in Fig. 4.

The thermal transition behaviors of all polymers during second heating process are summarized in Table 2. The mesophase to isotropization temperatures of 4M and 6M are significantly lower than those of 4H and 6H, respectively. This means that the randomly positioned methyl side-pendant group on hydroquinone units significantly destabilizes the mesophase. At the same time it makes the crystallization rates extremely slow. So, upon 10°C/min cooling, no crystallization peak is observed in DSC results. In our earlier articles of poly(ester-imide) made from *N*-(4-carboxybutyl) trimellitic imide and 2,6-diacetoxynaphthalene, the isotropization temperature was 343°C, which is higher than 4H by 75°C [10]. On the contrary, the crystal melting temperature (251°C) does not show much difference. It can be understood that as the naphthalene unit gives more rigidity to the molecular chain than the hydroquinone unit of 4H, the mesophase stable temperature range

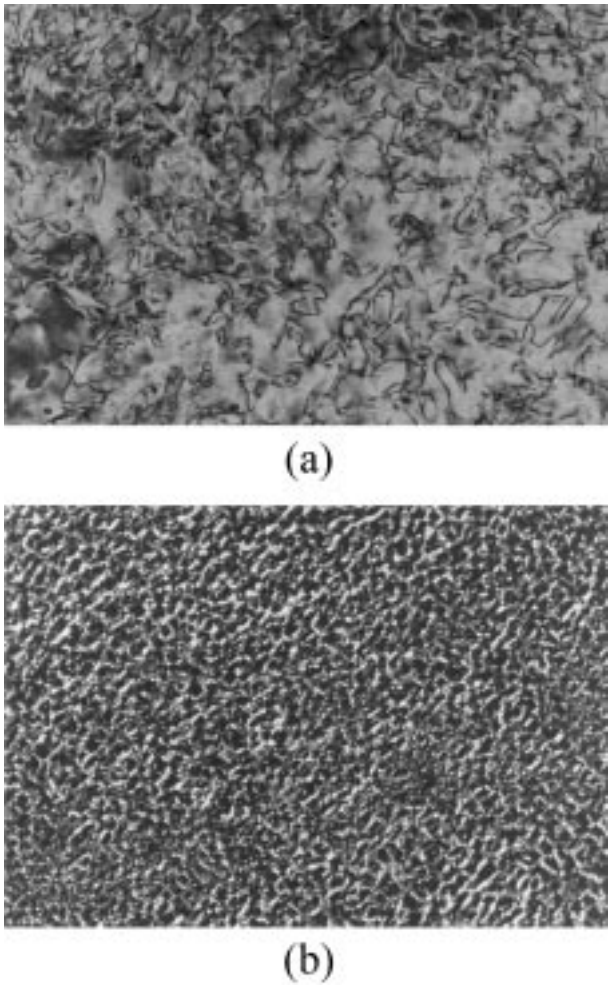

Fig. 4. Polarized light micrographs of 4M: (a) at 232°C; and (b) 203°C.

is broader. But the kink structure of naphthalene disturbs the crystallization of the polymer.

3.3. Crystallization velocity and phase structure

In the cases of 4M and 6M no crystallization behavior was observed in the dynamic DSC measurements. To know crystallization velocity, the polymers are annealed at various temperatures between the glass transition and the mesophase to isotropic phase transition. Fig. 5 shows the results of 6M. The isothermal annealing was immediately followed by the DSC heating scans. One can find two endotherms around 153 and 163°C. The crystallization

Table 2
Thermal transitions of all prepared poly(ester-imide)s during 10°C/min second heating

Polymer	T_g (°C)	T_m (°C) (ΔH_m(kcal/mru))	T_I (kcal/mru)(ΔH_i(kcal/mru))
4H	82.63	220.65 (0.69)	267.95 (0.98)
6H	72.63	220.90 (0.95)	252.92 (1.06)
4M	75.76	–	228.71 (0.68)
6M	57.21	–	185.17 (0.91)

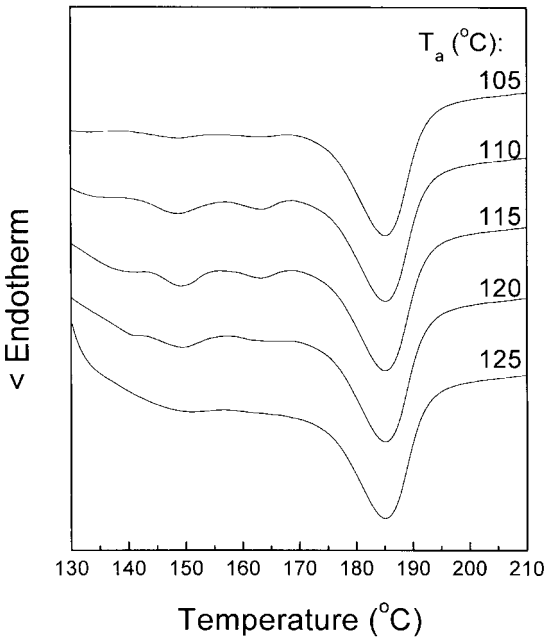

Fig. 5. DSC heating scans of 6M immediately after isothermal annealing at various temperature for 12 h. The heating rates were 10°C/min.

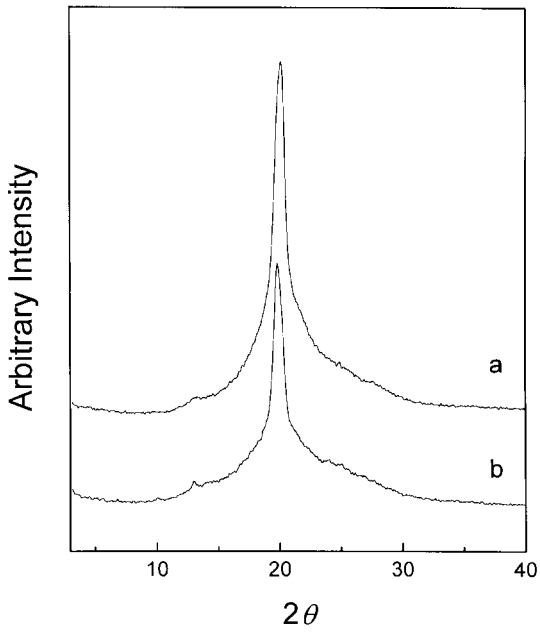

Fig. 7. WAXD diffractograms of 4H and 6H: (a) 6H; and (b) 4H. All samples were air-cooled from the temperatures above crystal melting.

velocity is the fastest around the annealing temperature of 110–115°C. But the crystallization velocity of 6M is so slow that the heat of fusion of the melting transition is only about 0.11 kcal/mru for the fastest crystallization velocity. On the other hand, 4M did not crystallize for all temperatures. It has been known that the crystallization rates of semiflexible type thermotropic polymers are usually slower with shorter methylene spacers. Fig. 6 is the DSC scan results after annealing at 112°C for various times. The result of 12 h annealing shows two melting endotherms. But another endotherm develops around 138°C at other annealing times. After 24 h, the growth rate slows down and after 36 h the endotherms do not grow anymore.

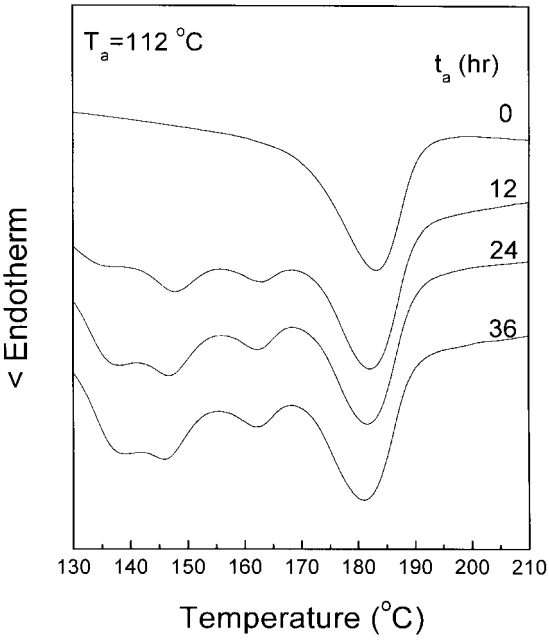

Fig. 6. DSC heating scans of 6M immediately after isothermal annealing at 112°C for various times. The heating rates were 10°C/min.

Fig. 7 shows the WAXD diffractograms of 4H and 6H. Samples were molded above their melting temperatures and then air-cooled. The crystal peak developed prominently due to fast crystallization of the polymers. The results from both polymers show a sharp crystal peak around $2\theta = 20°$, which illustrates the hexagonal lateral packing [21]. Even when the samples are quenched in liquid nitrogen, the diffractograms without crystal peaks were hard to obtain. Because the diffractograms of pure mesophase cannot be obtained, the exact classes of the mesophases are not known with the WAXD results. It will be discussed in the rheological measurement section.

Fig. 8 shows the WAXD diffractograms of 4M and 6M samples prepared in various conditions. The polymers do not crystallize when molded above their mesophase to isotropic phase transition temperature and air-cooled (Fig. 8c and d). As a result of their slow crystallization behavior we can obtain the typical nematic glassy patterns (without low angle peaks) under conventional cooling conditions. The WAXD patterns of 36 and 24 h annealed samples of 6M are shown in Fig. 8a and b, respectively. The annealing temperature is 112°C. Crystal peaks are seen in these cases. But the fraction of the crystal peaks to amorphous halo are smaller than those of 6H and 4H in Fig. 7, which means a low degree of crystallinity of the polymer after completion of the crystallization process.

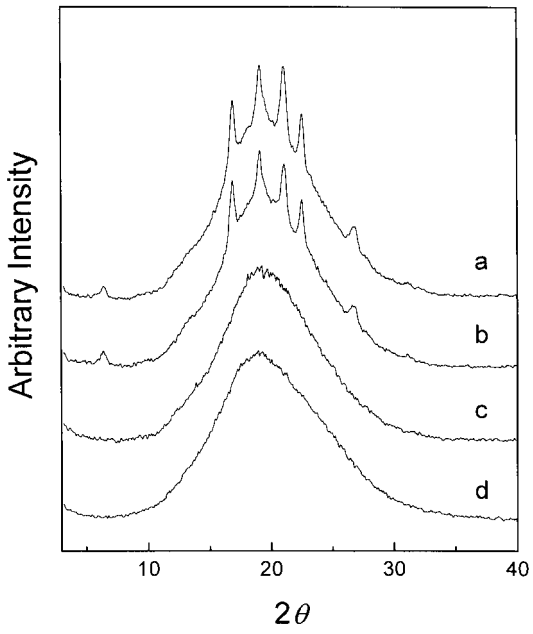

Fig. 8. WAXD diffractograms of 4M and 6M: (a) 6M after annealed at 112°C for 36 h and quenched in liquid nitrogen; (b) 6M after annealed at 112°C for 24 h and quenched in liquid nitrogen; (c) 6M after air-cooled from isotropic melt; and (d) 4M after air-cooled from isotropic melt.

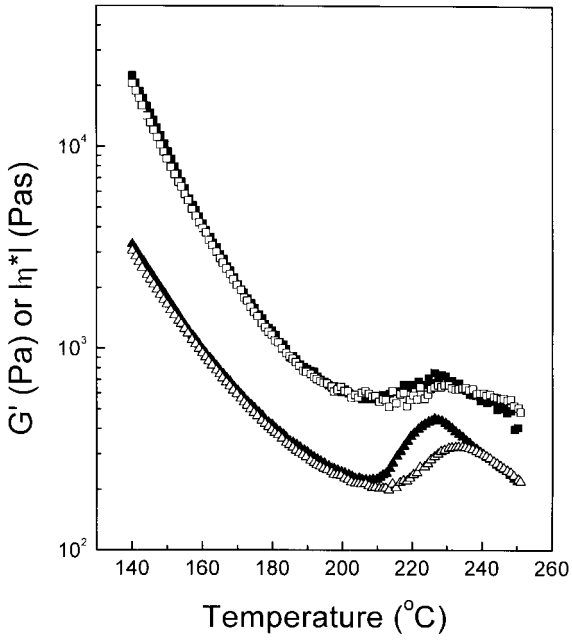

Fig. 9. Temperature sweep measurements of elastic modulus (□) and complex viscocity (△) for 4M. The closed symbols stand for cooling and the open symbols for heating. The scanning rate was 1°C/min. Gap setting was done at 200°C, strain was 0.1 and angular frequency was 10 rad/s.

3.4. Rheological characteristics

It has been known that polymers in mesophase show some unique features. So rheological methods can be used to check mesophase transition behaviors. Fig. 9 shows the elastic modulus and complex viscosity change of 4M on cooling and heating scans with scan rates of 1°C/min. The gap setting was done at 200°C. A disk shape sample was loaded at 250°C. After loading, the cooling scan was performed from loading temperature to 140°C and immediately followed by the heating scan on the same temperature region. A peak shape (sudden drop during cooling or sudden rise during heating) of storage modulus and complex viscosity is seen around 225°C, which agrees well with the mesophase to isotropic transition temperature of this polymer on DSC scan. The transition shape is a typical evidence of a nematic to isotropic phase transition [22,23]. More ordered smectic phases are known to show higher viscosity values than an isotropic phase [14,15,24]. Below the nematic to isotropic phase transition, the viscoelastic properties show good agreement during cooling and heating, which means no crystallization and corresponding melting transition.

Fig. 10a and b show the elastic modulus and complex viscosity curves and tan δ curve with temperature for 6M. The gap setting temperature was 160°C. The modulus and viscosity shapes are similar to those of 4M. Around 185°C peak shapes are seen. The tan δ curve shows a local minimum around the peak temperatures of modulus and viscosity. One can find that the viscoelastic properties of cooling and heating scan show less agreement than those of 4M in the nematic temperature region. The disagreement may be originated from the slow geometry relaxation during dynamic scans. Low nematic to isotropic phase transition temperature and high molecular weight of 6M can induce the slow relaxation of the geometry.

Fig. 11 shows the results of elastic modulus and complex viscosity of 6H. The gap setting was done at 220°C. The cooling and heating rate of 10°C/min was chosen to compare with the results of DSC. Peak shapes are also seen for this polymer around 240°C. The temperature agrees well with the mesophase to isotropic phase transition temperature obtained on 10°C/min DSC scans. So we can identify the mesophase of 6H as a nematic one. During cooling, modulus and viscosity values rise more than 2 decades around 200°C. On subsequent heating, the high values of modulus and viscosity are sustained to about 220°C and decrease to meet the values of cooling scan.

Frequency sweep measurements were performed for 6M. The temperature range was 140–200°C, which involves the nematic to isotropic phase transition region. For the measurements in biphase or nematic phase, samples were loaded at 180°C and cooled to measuring temperature in order to remove the shear history effect during squeezing of the samples in mesophase range. However, in spite of such heat treatment, the normal stress did not relax completely in 30 min or longer below 180°C. To attain reproducibility each measurement was repeated at least 3 times. Before each measurement, strain sweep measurements were performed to check the linear viscoelastic range. The linear viscoelastic limit was 0.05–0.08 in isotropic melt and

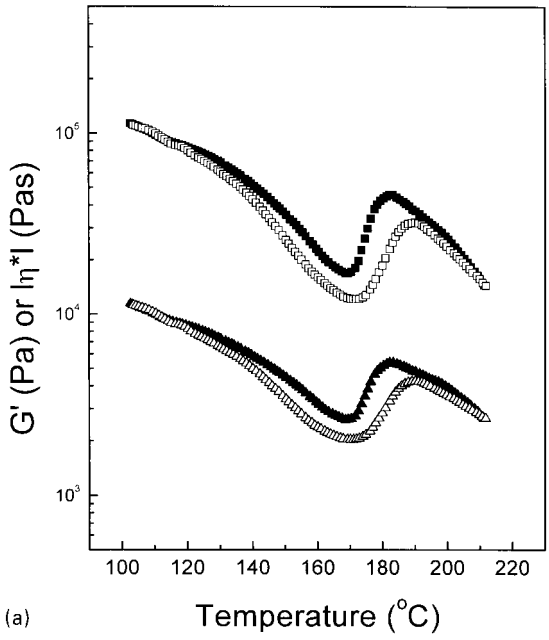

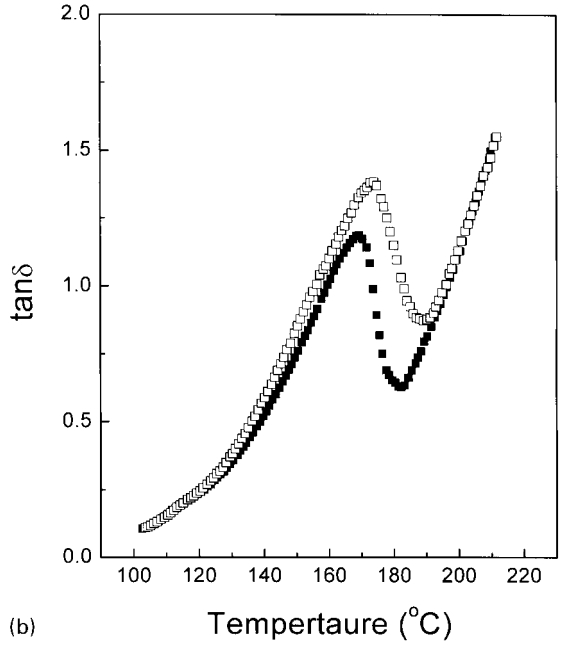

Fig. 10. Temperature sweep measurements of: (a) elastic modulus (□) and complex viscosity (△); and (b) tan δ for 6M. The closed symbols stand for cooling and the open symbols for heating. The scanning rate was 1°C/min. Gap setting was done at 160°C, strain was 0.1 and angular frequency was 10 rad/s.

0.02–0.04 in nematic mesophase. The tested frequency range was from 0.05 or 0.1 to 100 rad/s. The temperature dependency of complex viscosity is shown in Fig. 12. The results at 0.1, 1, 10, and 100 rad/s are plotted. Abrupt increase of viscosity is shown in the interval of 165–180°C for all frequencies. The extent of increase is wider in lower frequencies. From the results, it is seen that the polymer is isotropic at 180–200°C and nematic below

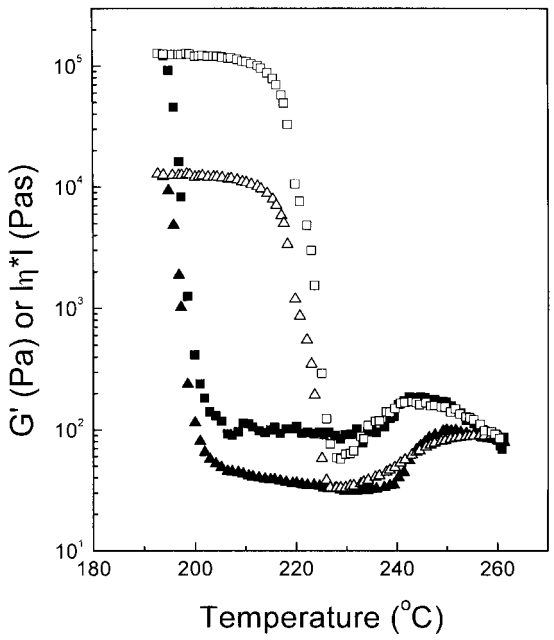

Fig. 11. Temperature sweep measurements of elastic modulus (□) and complex viscosity (△) for 6H. The closed symbols stand for cooling and the open symbols for heating. The scanning rate was 1°C/min. Gap setting was done at 220°C, strain was 0.1 and angular frequency was 10 rad/s.

165°C. The values between 165 and 180°C are in the transition region, which means that 6M is in biphase.

The time–temperature superposition is tested with the frequency sweep measurements results. Fig. 13a shows the results of 180–200°C. The reference temperature was 200°C. All curves are superposed very well in the temperature region, which is the typical result of an isotropic

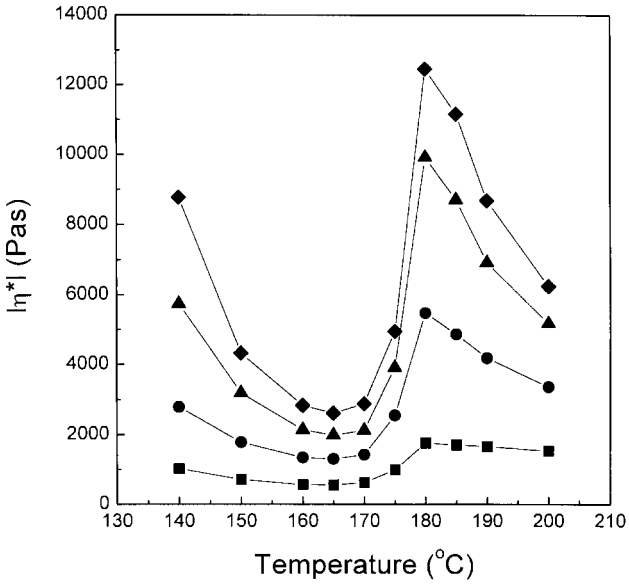

Fig. 12. Temperature dependencies of complex viscosity for 6H at various angular frequencies: ◆ 0.1 rad/s; ▲ 1 rad/s; ● 10 rad/s; and ■ 100 rad/s. Each strain was in linear viscoelasticity.

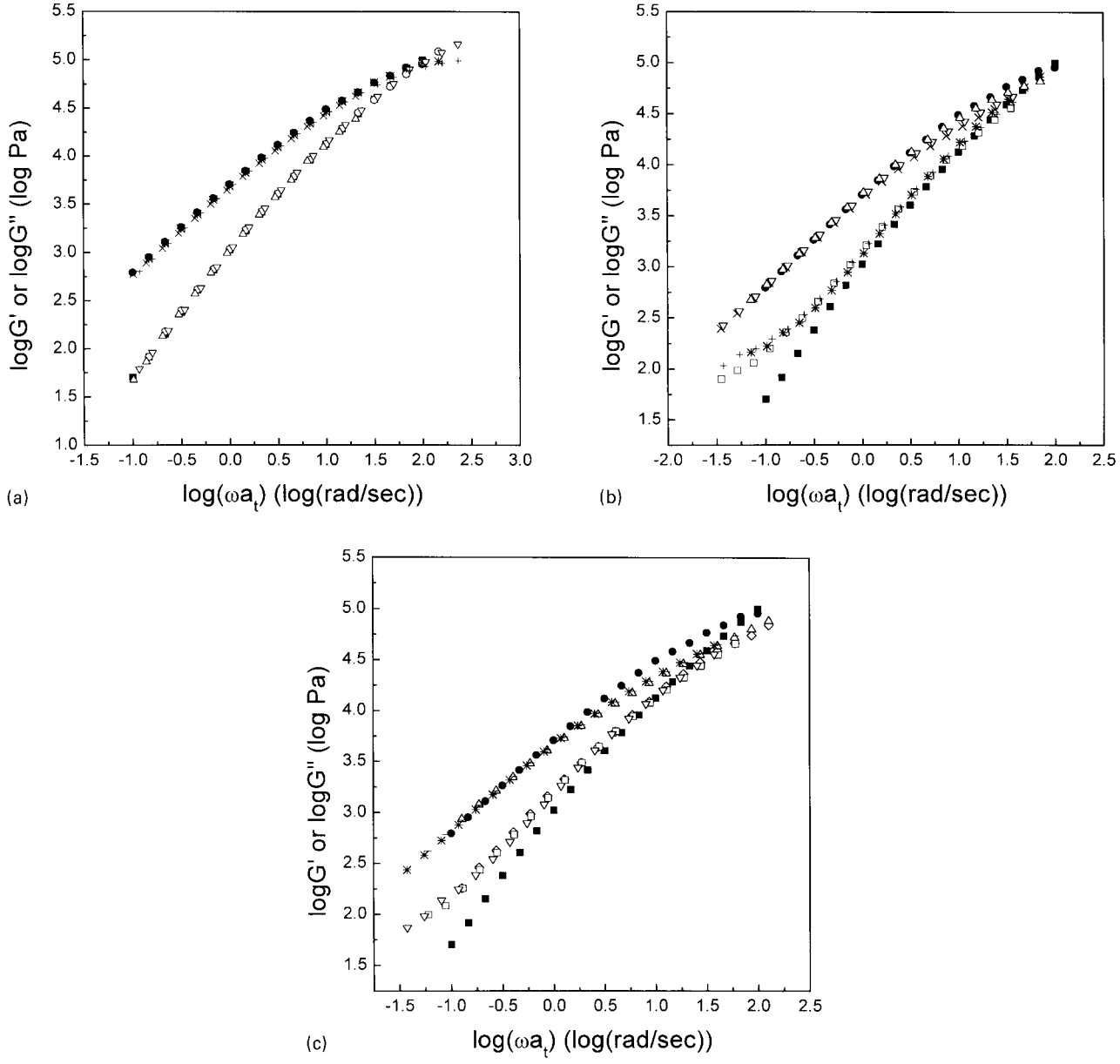

Fig. 13. Time temperature superposition results of elastic moduli, G', and loss moduli, G'', of 6M: (a) 180–200°C; (b) 165–175°C; and (c) 140–160°C. G': ■ 200°C, ○ 190°C, △ 185°C, ▽ 180°C, ∗ 175°C, + 170°C, □ 165°C, ▽ 160°C, □ 150°C and ○ 140°C; G'': ● 200°C, ∗ 190°C, × 185°C, + 180°C, △ 175°C, ▽ 170°C, × 165°C, ∗ 160°C, — 150°C and △ 140°C. A reference temperature is 200°C.

polymer melt. Together with the results shown in Fig. 12, one can find that 6M shows an isotropic phase above 180°C. The terminal slopes of elastic modulus and loss modulus are 1.33 and 0.92, respectively. The deviation from the typical terminal slope value, 2 for elastic modulus and 1 for loss modulus, may be originated from the broad molecular weight distribution of the polymer [24]. The transesterification reaction can bring out a wide molecular weight distribution. WLF equation fitting of shift factors with a reference temperature of 200°C yields $C_1 = 6.04$ and $C_2 = 350.67$.

Fig. 13b and c show the time–temperature superposition results of 6M below 180°C. The curves measured at 200°C are added for comparison. The superposition was performed for the best fit of loss modulus terminal to that of 200°C. As shown in Fig. 13b, superposition fails in biphasic region. Loss moduli deviate from the curve of 200°C in high-reduced frequency range. As the measurement temperature gets lower (closer to nematic region), the extent of deviation becomes larger. Elastic moduli deviate in all reduced frequency regions. The slopes of curves change following the 's' shape in the low-reduced frequency region. Fig. 13c shows the results in the nematic region. The curves of elastic and loss moduli in nematic phase show the deviation from the curves of 200°C but superpose well compared with those in the biphasic state in Fig. 13b. WLF equation fitting is

successful in the nematic phase as well. $C_1 = 5.36$ and $C_2 = 261.64$ are obtained with a reference temperature of 160°C. It has been reported that, for nematic side chain polymers, the superposition succeeded in both nematic and isotropic phases [25,26] but failed in biphase [26]. Success or failure of superposition has been reported for main chain liquid crystalline polymers by various groups [14,15,22,27]. The s-shaped curve of elastic moduli in low reduced frequency region is also shown in nematic state. It can be suggested that the s-shapes of elastic moduli in both biphase and nematic phase result from the domain structure. A similar non-terminal response of moduli was reported for a nematic polyether by Gillmor et al. [22]. They noted that the origin of the behavior was a structure in the material, which was larger than macromolecular dimensions.

4. Conclusion

Poly(ester-imide)s were prepared from *N*-(ω-carboxyalkylene) trimellitimides and hydroquinone diacetate or methylhydroquinone diacetate. Poly(ester-imide)s without methyl side-pendant group showed typical phase behaviors of enantiotropic liquid crystal polymer, i.e. glass transition, crystal melting transition(s) and isotropization transition on DSC heating scan. Their crystallization velocities were very fast. Even when quenched in liquid nitrogen, an uncrystallized sample was hard to obtain. Poly(ester-imide)s with methyl side group also showed mesophase but did not crystallize during the conventional cooling process. The nematic–glassy phases were easily obtained under usual cooling conditions. The crystallization velocities of the polymers were so slow that the completion of crystallization takes 32 h in the fastest case. On the temperature sweeps of viscoelastic properties, all polymers showed modulus and viscosity drops at the mesophase to isotropic phase transition, which means all polymers show nematic phase. For 6M, showing low mesophase to isotropic phase transition and slow crystallization, the dynamic rheological measurements are performed around the nematic to mesophase transition. The complex viscosity exhibited a sudden increase with temperature from 165 to 180°C, which means biphasic features around the temperatures. The lower the measuring frequencies, the larger the extent of increase of the complex viscosities. The time–temperature superposition succeeded within the modulus curves measured in nematic phase but failed in biphase.

Acknowledgements

This work was financially supported by the Korea Science and Engineering Foundation, KOSEF, under contract 971-0804-039-2.

References

[1] Jackson Jr WJ, Kuhfuss HJ. J Polym Sci Polym Chem 1976;14:2043–58.
[2] Griffin AC, Havens SJ. J Polym Sci Polym Phys 1981;19:951–69.
[3] Antoun S, Lenz RW, Jin JI. J Polym Sci Polym Chem 1981;19:1901–20.
[4] Blumstein A, Vilasagar S, Ponrathnam S, Clough SB, Blumstein RB. J Polym Sci Polym Phys 1982;20:877–92.
[5] Asrar J, Toriumi H, Watanabe J, Krigbaum WR, Ciferri A. J Polym Sci Polym Phys 1983;21:1119–31.
[6] Aharoni SM. Macromolecules 1988;21:1941–61.
[7] Percec V, Yourd R. Macromolecules 1989;22:524–37.
[8] Percec V, Yourd R. Macromolecules 1989;22:3229–42.
[9] Kricheldorf HR. Adv Polym Sci 1999;141:83–188.
[10] Kim TK, Kim SO, Chung IJ. Polym Adv Technol 1997;8:305–18.
[11] Kim TK, Kim KK, Chung IJ. Polym J 1997;29:85–94.
[12] Bello A, Perez E, Marugan MM, Perena JM. Macromolecules 1990;23:907–10.
[13] Perez E, Benavente R, Bello A, Perena JM, VanderHart DL. Macromolecules 1995;28:6211–8.
[14] Hudson SD, Lovinger AJ, Larson RG, Davis DD, Garay RO, Fujishiro. Macromolecules 1993;26:5643.
[15] Alt DJ, Hudson SD, Garay RO, Fujishiro K. Macromolecules 1995;28:1575–9.
[16] Assman K, Schneider HA, Kricheldorf HR. Mol Cryst Liq Cryst 1993;231:29–44.
[17] Chang S, Han CD. Macromolecules 1996;29:2383–91.
[18] Chang S, Han CD. Macromolecules 1997;30:1656–69.
[19] Kricheldorf HR, Pakull R, Buchner S. J Polym Sci Polym Chem 1989;27:431–46.
[20] Ge JJ, Zhang A, McCreight KW, Ho RM, Wang SY, Jin X, Harris FW, Cheng SZD. Macromolecules 1997;30:6498–506.
[21] Pardey R, Wu SS, Chen J, Harris FW, Cheng SZD, Keller A, Aducci J, Facinelli JV, Lenz RW. Macromolecules 1994;27:5794–802.
[22] Gillmor JR, Colby RH, Hall E, Ober CK. J Rheol 1994;38:1623–38.
[23] Kalika DS, Shen MR, Yu XM, Denn MM, Ianelli P, Masciocchi N, Yoon DY, Parrish W, Friedrich C, Noel C. Macromolecules 1990;23:5192–200.
[24] Ferry JD. Viscoelastic properties of polymers, 3. New York: Wiley, 1980. p. 387–91.
[25] Kannan RM, Kornfield JA, Schwenk N, Boeffel C. Macromolecules 1993;26:2050–6.
[26] Berghausen J, Fuchs J, Richtering W. Macromolecules 1997;30:7574–81.
[27] Graziano DJ, Mackley MR, Wissbrun KF. J Non-Newt Fluid Mech 1983;13:243–57.